ELSEVIER

Comput. Methods Appl. Mech. Engrg. 154 (1998) 281–297

Computer methods in applied mechanics and engineering

A multiscale finite element method for the Helmholtz equation

Assad A. Oberai[1], Peter M. Pinsky*,[2]

Division of Applied Mechanics, Stanford University, Stanford, CA 94305-4040, USA

Received 25 June 1996

Abstract

It is well known that when the standard Galerkin method is applied to the Helmholtz equation it exhibits an error in the wavenumber and the solution does not, therefore, preserve the phase characteristics of the exact solution. Improvements on the Galerkin method, including Galerkin least-squares (GLS) methods, have been proposed. However, these approaches rely on a dispersion analysis of the underlying difference stencils in order to reduce error in the solution. In this paper we propose a multiscale finite element for the Helmholtz equation. The method employs a multiscale variational formulation which leads to a subgrid model in which subgrid scales are incorporated analytically through appropriate Green's functions. It is shown that entirely new and accurate methods emerge and that GLS methods can be obtained as special cases of the more general subgrid model. © 1998 Elsevier Science S.A.

1. Introduction

Time-harmonic problems of acoustic radiation and scattering are governed by the Helmholtz equation in the fluid domain, coupled to the structural equations for elastic bodies in contact with the fluid. Solutions in the fluid domain describe propagating and evanescent waves and have been approximated by finite difference, finite element and boundary element methods. In the case of exterior problems the domain-based finite difference and finite element methods will employ a suitable radiation boundary condition on the truncated fluid domain, or in the case of finite elements may be coupled with infinite elements. In this paper we are concerned with developing a new multiscale finite element method for acoustic wave propagation in the fluid domain governed by the Helmholtz equation. The development of this method also serves as a model for a parallel development that could be undertaken for wave propagation in the elastic solid.

It is well known that the accuracy of the solutions to the Helmholtz equation obtained by the standard Galerkin finite element method deteriorates rapidly with increasing wavenumber. Errors inherent in the method result in numerical waves that propagate with a wavenumber k^h which is different to the acoustic wavenumber k. In fact it has been shown by Babuška, et al. [1] that the discretization error for the standard Galerkin finite element method is related to the absolute value of the difference in wavenumbers $k - k^h$. There have been efforts to formulate new methods which are designed to reduce the difference between k and k^h in order to improve accuracy.

The Galerkin least-squares (GLS) method [2,7] and the Generalized FEM [1] are two such methods. Both of these methods rely on the dispersion relation between k and k^h obtained from a discrete Fourier transform of the underlying finite-difference stencil of the respective numerical method, although they make use of this

* Corresponding author.

[1] Graduate Research Assistant.

[2] Professor of Mechanical Engineering.

PII S0045-7825(97)00130-8

relationship in quite distinct ways. The GLS method appends residuals of the Euler–Lagrange equations in a least-squares form to the Galerkin variational form using a local mesh parameter. For the Helmholtz equation in one dimension and under certain restrictions, an expression for the local mesh parameter has been determined from the condition that minimizes the difference between k and k^h [2]. Unfortunately, determining the local mesh parameter from this condition in multi-dimensions is problematic [7] and suggests that a deeper understanding of how to apply so-called stabilized methods to acoustics is needed. Indeed, the very fact that the local mesh parameter must be solved from the dispersion relationship suggests that the resulting method will have inherent limitations for general problems.

Recently, a multiscale variational formulation for problems governed by general differential operators has been proposed by Hughes [3,4] who also illustrated how the approach can be used to construct new subgrid scale models for problems with multiscale phenomena. The multiscale variational formulation starts by the decomposition of the solution into two parts representing two disparate spatial scales. In the development of subgrid models from the multiscale variational form, these length scales are characterized with respect to the size of the numerical grid.

In this paper we propose a new finite element method for the Helmholtz equation based on the variational formulation developed by Hughes [4]. In particular, we assume a sum decomposition of the wave solution into a part which is resolvable by the grid and a part which is unresolvable, and is solved for analytically. The multiscale variational formulation is developed in its general form for the Helmholtz operator and for general boundary conditions. The unresolved scales are eliminated from the variational problem through the use of an appropriate Green's function resulting in a multiscale variational form expressed in terms of the resolvable scales only. By specializing the unresolved scales to be the finite scales in the solution, we then obtain a subgrid model for the Helmholtz equation.

The particular subgrid model developed in this paper results from a very strong assumption on the unresolved scales, namely that they vanish on element boundaries. It is shown that while this assumption leads to a numerical method that is nodally exact in one dimension, in multi-dimensions it limits the accuracy of the resulting subgrid model. Nevertheless, the general multiscale variational framework established here for the Helmholtz equation can be used for the development of further models that do not inherit the above limitation [5].

An outline of this paper is as follows. In Section 2 of this paper we derive the multiscale variational formulation for the Helmholtz equation. In Section 3, we develop a subgrid model from this formulation. For the details on the subgrid model the reader is referred to [3]. In Section 4, we construct a numerical method from this model and in Section 5, we prove superconvergence for this method in one dimension. In Section 6 we assess the performance of this new method and compare it with some other standard finite element methods.

2. Multiscale variational formulation

The strong statement of the problem we wish to solve is: Find $\phi: \Omega \to \mathbb{C}$, the spatial component of the acoustic pressure or the velocity potential in open bounded domain Ω with a smooth boundary Γ, such that

$$\mathcal{L}\phi = f \qquad \text{in } \Omega \tag{1}$$

$$\phi = q \qquad \text{on } \Gamma_q \tag{2}$$

$$\phi_{,n} = \nabla\phi \cdot \boldsymbol{n} = -\mathrm{i}k\phi + p \qquad \text{on } \Gamma_h \tag{3}$$

where $\mathcal{L} \equiv -\nabla^2 - k^2$ is the Helmholtz operator, $k \in \mathbb{R}$ is the wavenumber, $f: \Omega \to \mathbb{C}$ is the prescribed forcing function and $q: \Gamma_q \to \mathbb{C}$ is the prescribed Dirichlet boundary data. Eq. (3) is a mixed boundary condition on $\Gamma_h = \Gamma - \Gamma_g$, where $\boldsymbol{n}$ is the unit outward normal on the boundary Γ and $p: \Gamma_h \to \mathbb{C}$ is the prescribed Neumann data. Note that the Helmholtz operator $\mathcal{L}$ is self adjoint viz. $\mathcal{L} = \mathcal{L}^*$.

The equivalent weak statement of the Boundary Value Problem is: Find $\phi \in \mathcal{S}$ such that

$$a(w, \phi) + \mathrm{i}k(w, \phi)_{\Gamma_h} = (w, f) + (w, p)_{\Gamma_h} \quad \forall\, w \in \mathcal{V} \tag{4}$$

where we define the function spaces $\mathcal{S}$ and $\mathcal{V}$ as

$$\mathcal{S} = \{\phi \,|\, \phi \in H^1(\Omega),\ \phi = q \text{ on } \Gamma_q\} \tag{5}$$

$$\mathcal{V} = \{w \,|\, w \in H^1(\Omega),\ w = 0 \text{ on } \Gamma_q\} \tag{6}$$

The sesquilinear form $a(\cdot,\cdot)$: $\mathcal{V} \times \mathcal{S} \to \mathbb{C}$ is defined as

$$a(w, \phi) := (\nabla w, \nabla \phi) - k^2 (w, \phi) \tag{7}$$

And the inner products $(\cdot,\cdot)$ and $(\cdot,\cdot)_{\Gamma_h}$ are defined as

$$(w, \phi) := \int_\Omega w^* \phi \, d\Omega \tag{8}$$

$$(w, \phi)_{\Gamma_h} := \int_{\Gamma_h} w^* \phi \, d\Gamma \tag{9}$$

where w^* denotes the complex conjugate of w.

From the weak statement of the BVP (4) we now derive a multiscale variational formulation for this problem. This derivation closely follows the steps outlined in [4]. We begin by discretizing the domain Ω into element subdomains Ω^e with boundary Γ^e, $e = 1, 2, \ldots, n_{el}$, where n_{el} is the number of elements. Let

$$\Omega' = \bigcup_{n=1}^{n_{el}} \Omega_n \qquad \text{(Element interiors)} \tag{10}$$

$$\Gamma' = \bigcup_{n=1}^{n_{el}} \Gamma_n - \Gamma \quad \text{(Element interiors)} \tag{11}$$

$$\overline{\Omega} = \overline{\Omega}' = \text{closure}(\Omega') \tag{12}$$

Then, we consider the following sum decomposition of ϕ and w.

$$\phi = \overline{\phi} + \phi' \tag{13}$$

$$w = \overline{w} + w' \tag{14}$$

where $\overline{\phi} \in \overline{\mathcal{S}}$, $\phi' \in \mathcal{S}'$, $\overline{\omega} \in \overline{\mathcal{V}}$ and $w' \in \mathcal{V}'$. Further $\mathcal{S} = \overline{\mathcal{S}} \oplus \mathcal{S}'$ and $\mathcal{V} = \overline{\mathcal{V}} \oplus \mathcal{V}'$. In the decomposition ϕ' and $\overline{\phi}$ are chosen to represent two disparate scales in the problem. The variational equation (4) may now be written as

$$a(\overline{w} + w', \overline{\phi} + \phi') + ik(\overline{w} + w', \overline{\phi} + \phi')_{\Gamma_h} = (\overline{w} + w', f) + (\overline{w} + w', p)_{\Gamma_h} \tag{15}$$

This leads to the following two sub-problems

$$a(\overline{w}, \overline{\phi}) + ik(\overline{w}, \overline{\phi})_{\Gamma_h} + a(\overline{w}, \phi') + ik(\overline{w}, \phi')_{\Gamma_h} = (\overline{w}, f) + (\overline{w}, p)_{\Gamma_h} \tag{16}$$

and

$$a(w', \overline{\phi}) + ik(w', \overline{\phi})_{\Gamma_h} + a(w', \phi') + ik(w', \phi')_{\Gamma_h} = (w', f) + (w', p)_{\Gamma_h} \tag{17}$$

Upon integrating by parts in the sesquilinear forms $a(\overline{w}, \phi')$, $a(w', \overline{\phi})$ and $a(w', \phi')$ we obtain

$$\begin{aligned} a(\overline{w}, \phi') &= (\mathcal{L}\overline{w}, \phi')_{\Omega'} + ([\![\overline{w}_{,n}]\!], \phi')_{\Gamma'} + (\overline{w}_{,n}, \phi')_{\Gamma_h} \\ &= (\mathcal{L}\overline{w}, \phi')_{\Omega} + (\overline{w}_{,n}, \phi')_{\Gamma_h} \end{aligned} \tag{18}$$

$$\begin{aligned} a(w', \overline{\phi}) &= (w', \mathcal{L}\overline{\phi})_{\Omega'} + (w', [\![\overline{\phi}_{,n}]\!])_{\Gamma'} + (w', \overline{\phi}_{,n})_{\Gamma_h} \\ &= (w', \mathcal{L}\overline{\phi})_{\Omega} + (w', \overline{\phi}_{,n})_{\Gamma_h} \end{aligned} \tag{19}$$

$$\begin{aligned} a(w', \phi') &= (w', \mathcal{L}\phi')_{\Omega'} + (w', [\![\phi'_{,n}]\!])_{\Gamma'} + (w', \phi'_{,n})_{\Gamma_h} \\ &= (w', \mathcal{L}\phi')_{\Omega} + (w', \phi'_{,n})_{\Gamma_h} \end{aligned} \tag{20}$$

where $[\![\cdot]\!]$ is used to denote the jump in a variable across element boundaries and the inner products $(\cdot,\cdot)_{\Omega'}$ and $(\cdot,\cdot)_{\Gamma'}$ are defined as

$$(w,\phi)_{\Omega'} := \int_{\Omega'} w^*\phi \,\mathrm{d}\Omega \tag{21}$$

$$(w,\phi)_{\Gamma'} := \int_{\Gamma'} w^*\phi \,\mathrm{d}\Gamma \tag{22}$$

It may be noted that the terms $\mathscr{L}\bar{w}$, $\mathscr{L}\phi'$ and $\mathscr{L}\bar{\phi}$ are Dirac distributions on Ω. Using Eq. (18) in Eq. (16) we obtain for the first sub-problem

$$a(\bar{w},\bar{\phi}) + \mathrm{i}k(\bar{w},\bar{\phi})_{\Gamma_h} + (\mathscr{L}\bar{w},\phi') + (\bar{w}_{,n} + \mathrm{i}k\bar{w},\phi')_{\Gamma_h} = (\bar{w},f) + (\bar{w},p)_{\Gamma_h} \tag{23}$$

And using Eqs. (19) and (20) in Eq. (17) we obtain for the second subproblem

$$(w',\mathscr{L}\bar{\phi} + \mathscr{L}\phi') + (w',\bar{\phi}_{,n} + \mathrm{i}k\bar{\phi} + \phi'_{,n} + \mathrm{i}k\phi')_{\Gamma_h} = (w',f) + (w',p)_{\Gamma_h} \tag{24}$$

For the case when $\mathscr{V}'$ and $\bar{\mathscr{V}}$ are orthogonal with respect to the $L_2(\Omega)$ inner product, we define $\Pi' : \mathscr{V} \to \mathscr{V}'$ to be the orthogonal projection of $\mathscr{V}$ onto $\mathscr{V}'$. The Euler–Lagrange equations for the second sub-problem yield

$$\Pi'\mathscr{L}\phi' = -\Pi'(\mathscr{L}\bar{\phi} - f) \qquad \text{in } \Omega \tag{25}$$

$$\phi' = 0 \qquad \text{on } \Gamma_q \tag{26}$$

$$\phi'_{,n} = -\mathrm{i}k\phi' - (\bar{\phi}_{,n} + \mathrm{i}k\bar{\phi} - p) \qquad \text{on } \Gamma_h \tag{27}$$

The relevant Green's function problem corresponding to (25), (26) and (27) is

$$\Pi'\mathscr{L}^*g'(\boldsymbol{x};\boldsymbol{x}_0) = \Pi'\mathscr{L}g(\boldsymbol{x};\boldsymbol{x}_0) = \Pi'\delta(\boldsymbol{x}-\boldsymbol{x}_0) \quad \text{in } \Omega \tag{28}$$

$$g'(\boldsymbol{x};\boldsymbol{x}_0) = 0 \qquad \text{on } \Gamma_q \tag{29}$$

$$g'(\boldsymbol{x};\boldsymbol{x}_0)_{,n_x} = -\mathrm{i}kg'(\boldsymbol{x};\boldsymbol{x}_0) \qquad \text{on } \Gamma_h \tag{30}$$

Thus

$$\begin{aligned}\phi'(\boldsymbol{x}_0) &= -\int_{\Omega} g'(\boldsymbol{x};\boldsymbol{x}_0)(\mathscr{L}\bar{\phi} - f)(\boldsymbol{x})\,\mathrm{d}\Omega_x - \int_{\Gamma_h} g'(\boldsymbol{x};\boldsymbol{x}_0)(\bar{\phi}_{,n} + \mathrm{i}k\bar{\phi} - p)(\boldsymbol{x})\,\mathrm{d}\Gamma_x \\ &= -\int_{\Omega'} g'(\boldsymbol{x};\boldsymbol{x}_0)(\mathscr{L}\bar{\phi} - f)(\boldsymbol{x})\,\mathrm{d}\Omega_x - \int_{\Gamma'} g'(\boldsymbol{x};\boldsymbol{x}_0)([\![\bar{\phi}_{,n}]\!])(\boldsymbol{x})\,\mathrm{d}\Gamma_x \\ &\quad - \int_{\Gamma_h} g'(\boldsymbol{x};\boldsymbol{x}_0)(\bar{\phi}_{,n} + \mathrm{i}k\bar{\phi} - p)(\boldsymbol{x})\,\mathrm{d}\Gamma_x \\ &= M(\bar{\phi},f)\end{aligned} \tag{31}$$

The first sub-problem (23) may now be written completely in terms of $\bar{\phi}$ as

$$a(\bar{w},\bar{\phi}) + \mathrm{i}k(\bar{w},\bar{\phi})_{\Gamma_h} + (\mathscr{L}\bar{w}, M(\bar{\phi},f)) + (\bar{w}_{,n} + \mathrm{i}k\bar{w}, M(\bar{\phi},f))_{\Gamma_h} = (\bar{w},f) + (\bar{w},p)_{\Gamma_h} \tag{32}$$

where

$$\begin{aligned}(\mathscr{L}\bar{w}, M(\bar{\phi},f)) &= -\int_{\Omega} \mathscr{L}\bar{w}^*(\boldsymbol{x}_0)M(\bar{\phi},f)(\boldsymbol{x}_0)\,\mathrm{d}\Omega_{x_0} \\ &= -\int_{\Omega'} \mathscr{L}\bar{w}^*(\boldsymbol{x}_0)M(\bar{\phi},f)(\boldsymbol{x}_0)\,\mathrm{d}\Omega_{x_0} - \int_{\Gamma'} [\![\bar{w}^*_{,n}]\!](\boldsymbol{x}_0)M(\bar{\phi},f)(\boldsymbol{x}_0)\,\mathrm{d}\Gamma_{x_0}\end{aligned} \tag{33}$$

and $M(\bar{\phi},f)$ is defined in Eq. (31). Eq. (32) is the statement of the *multiscale variational formulation* for the BVP given by Eqs. (1) through (3).

REMARKS

(1) The multiscale variational formulation (32) is an equation for $\bar{\phi}$ that exactly accounts for the effect of ϕ' on $\bar{\phi}$.

(2) If we consider a BVP with only Dirichlet boundary conditions then the multiscale variational formulation (32) simplifies to

$$a(\bar{w}, \bar{\phi}) + (\mathcal{L}\bar{w}, M(\bar{\phi}, f)) = (\bar{w}, f) \tag{34}$$

where

$$\begin{aligned}(\mathcal{L}\bar{w}, M(\bar{\phi}, f)) &= -\int_{\Omega}\int_{\Omega} \mathcal{L}\bar{w}^*(\boldsymbol{x}_0) g'(\boldsymbol{x}; \boldsymbol{x}_0)(\mathcal{L}\bar{\phi} - f)(\boldsymbol{x})\, d\Omega_x\, d\Omega_{x_0} \\ &= -\int_{\Omega'}\int_{\Omega'} \mathcal{L}\bar{w}^*(\boldsymbol{x}_0) g'(\boldsymbol{x}; \boldsymbol{x}_0)(\mathcal{L}\bar{\phi} - f)(\boldsymbol{x})\, d\Omega_x\, d\Omega_{x_0} \\ &\quad - \int_{\Omega'}\int_{\Gamma'} \mathcal{L}\bar{w}^*(\boldsymbol{x}_0) g'(\boldsymbol{x}; \boldsymbol{x}_0)[\![\bar{\phi}_{,n}]\!](\boldsymbol{x})\, d\Gamma_x\, d\Omega_{x_0} \\ &\quad - \int_{\Gamma'}\int_{\Omega'} [\![\bar{w}^*_{,n}]\!](\boldsymbol{x}_0) g'(\boldsymbol{x}; \boldsymbol{x}_0)(\mathcal{L}\bar{\phi} - f)(\boldsymbol{x})\, d\Omega_x\, d\Gamma_{x_0} \\ &\quad - \int_{\Gamma'}\int_{\Gamma'} [\![\bar{w}^*_{,n}]\!](\boldsymbol{x}_0) g'(\boldsymbol{x}; \boldsymbol{x}_0)[\![\bar{\phi}_{,n}]\!](\boldsymbol{x})\, d\Gamma_x\, d\Gamma_{x_0}\end{aligned} \tag{35}$$

which agrees with the result for a general second order differential operator given in [4]. Further, if we assume that the functions $\bar{\phi}$, ϕ', $\bar{w}$ and $w' \in C^1(\Omega)$ then the term $(\mathcal{L}\bar{w}, M(\bar{\phi}, f))$ in Eq. (34) simplifies to

$$(\mathcal{L}\bar{w}, M(\bar{\phi}, f)) = -\int_{\Omega'}\int_{\Omega'} \mathcal{L}\bar{w}^*(\boldsymbol{x}_0) g'(\boldsymbol{x}; \boldsymbol{x}_0)(\mathcal{L}\bar{\phi} - f)(\boldsymbol{x})\, d\Omega_x\, d\Omega_{x_0} \tag{36}$$

(3) The multiscale variational formulation (32) needs to be simplified by making certain assumptions on $\bar{\phi}$ and ϕ'. To implement a finite dimensional approximation of Eq. (32) would pose the following problems:
   (a) An a priori knowledge of the Green's function for the problem is required.
   (b) The integral operator M acting on $\bar{\phi}$ will couple all the degrees of freedom of $\bar{\phi}$ in the problem domain Ω.

   While it is useful to develop numerical methods based directly on some form of the multiscale variational formulation [5], in the following section we make an assumption on ϕ' and w' that removes the noted difficulties but which also imposes limitations on the resulting numerical method.

3. Subgrid model

In this section we develop a subgrid model for the Helmholtz equation following the procedure outlined in [3], for a general differential operator. The subgrid model can be thought of as a specialization of the more general multiscale variational equation derived in the previous section. In this model we characterize $\bar{\phi}$ and ϕ' with respect to the size of the numerical grid. We choose $\bar{\phi}$ to represent the resolved or the coarse scales and ϕ' to represent the unresolved or the fine scales (see Fig. 1). We then replace $\bar{\phi}$ and $\bar{\omega}$ with their finite-dimensional counterparts $\bar{\phi}^h$ ($\bar{\phi}^h \in \bar{\mathcal{S}}^h \subset \bar{\mathcal{S}}$) and $\bar{\omega}^h$ ($\bar{\omega}^h \in \bar{\mathcal{V}}^h \subset \bar{\mathcal{V}}$). The spaces $\bar{\mathcal{S}}^h$ and $\bar{\mathcal{V}}^h$ are chosen to precisely allow for piecewise linear, bilinear and trilinear finite element interpolation functions in one, two and three dimensions respectively. Further, as pointed out in the previous section we make the following assumption on ϕ' and w' that simplifies the multiscale variational formulation.

$$\phi' = 0 \quad \text{on } \Gamma' \cup \Gamma \tag{37}$$

$$w' = 0 \quad \text{on } \Gamma' \cup \Gamma \tag{38}$$

i.e. the subgrid scales vanish on element boundaries. We observe that w' and $\phi' \in \mathcal{V}'$, where $\mathcal{V}'$ is defined by

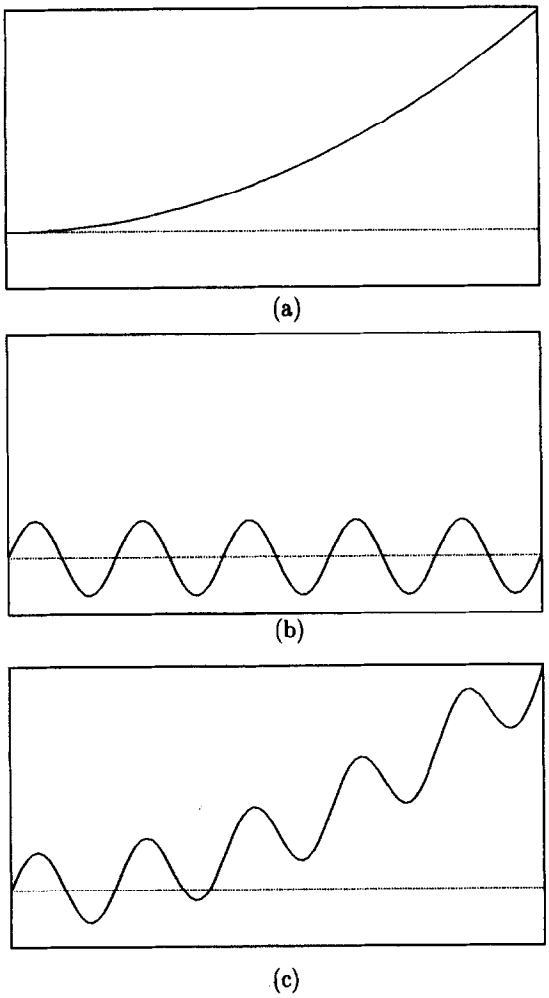

Fig. 1. (a) Resolvable scales; (b) unresolvable scales; (c) multiscale response.

$$\mathcal{V}' = \{w \mid w \in \mathcal{V} \backslash \overline{\mathcal{V}}^h, \quad w = 0 \text{ on } \Gamma' \cup \Gamma\} \tag{39}$$

Using Eqs. (37) and (38) in the expressions for the sesquilinear forms $a(\overline{w}^h, \phi')$, $a(w', \overline{\phi}^h)$ and $a(w', \phi')$ (Eqs. (18) through (20)) we obtain

$$a(\overline{w}^h, \phi') = (\mathcal{L}\overline{w}^h, \phi')_{\Omega'} \tag{40}$$

$$a(w', \overline{\phi}^h) = (w', \mathcal{L}\overline{\phi}^h)_{\Omega'} \tag{41}$$

$$a(w', \phi') = (w', \mathcal{L}\phi')_{\Omega'} \tag{42}$$

Using Eq. (40) in Eq. (16) we obtain for the first sub-problem

$$a(\overline{w}^h, \overline{\phi}^h) + ik(\overline{w}^h, \overline{\phi}^h)_{\Gamma_h} + (\mathcal{L}\overline{w}^h, \phi')_{\Omega'} = (\overline{w}^h, f) + (\overline{w}^h, p)_{\Gamma_h} \tag{43}$$

And using Eqs. (41) and (42) in Eq. (17) we obtain for the second sub-problem

$$(w', \mathcal{L}\overline{\phi}^h)_{\Omega'} + (w', \mathcal{L}\phi')_{\Omega'} = (w', f)_{\Omega'} \tag{44}$$

The Euler–Lagrange equations for the second sub-problem yield for each element $e = 1, 2, \ldots, n_{el}$

$$\mathcal{L}\phi' = -(\mathcal{L}\bar{\phi}^h - f) \quad \text{in } \Omega^e \tag{45}$$

$$\phi' = 0 \quad \text{on } \Gamma^e \tag{46}$$

The relevant Green's function problem corresponding to each of these problems is

$$\mathcal{L}g^e(\boldsymbol{x};\boldsymbol{x}_0) = \delta(\boldsymbol{x}-\boldsymbol{x}_0) \quad \text{in } \Omega^e \tag{47}$$

$$g^e(\boldsymbol{x};\boldsymbol{x}_0) = 0 \quad \text{on } \Gamma^e \tag{48}$$

Thus

$$\begin{aligned}\phi'^e := \phi'(\boldsymbol{x}_0)|_{\Omega^e} &= -\int_{\Omega^e} g^e(\boldsymbol{x};\boldsymbol{x}_0)(\mathcal{L}\bar{\phi}^h - f)(\boldsymbol{x})\,\mathrm{d}\Omega_x \\ &= M^e(\mathcal{L}\bar{\phi}^h - f)\end{aligned} \tag{49}$$

Using this expression for ϕ' in the first sub-problem we obtain the *subgrid model* for the Helmholtz equation, viz.

$$a(\bar{w}^h, \bar{\phi}^h) + \mathrm{i}k(\bar{w}^h, \bar{\phi}^h)_{\Gamma_h} + (\mathcal{L}\bar{w}^h, M(\mathcal{L}\bar{\phi}^h - f)) = (\bar{w}^h, f) + (\bar{w}^h, p)_{\Gamma_h} \tag{50}$$

where

$$\begin{aligned}(\mathcal{L}\bar{w}^h, M(\mathcal{L}\bar{\phi}^h - f)) &= \sum_{n=1}^{n_{\mathrm{el}}} (\mathcal{L}\bar{w}^h, M^e(\mathcal{L}\bar{\phi}^h - f))_{\Omega_e} \\ &= -\sum_{n=1}^{n_{\mathrm{el}}} \int_{\Omega_e}\int_{\Omega_e} \mathcal{L}\bar{w}^{h*}(\boldsymbol{x}_0) g^e(\boldsymbol{x};\boldsymbol{x}_0)(\mathcal{L}\bar{\phi}^h - f)(\boldsymbol{x})\,\mathrm{d}\Omega_x\,\mathrm{d}\Omega_{x_0}\end{aligned} \tag{51}$$

REMARKS

(1) The subgrid model (50) exactly accounts for the effect of the unresolved scales on the resolved scales up to the assumptions (37) and (38).

(2) Assumptions (37) and (38) imply that the non local effect of the resolved scales is confined to element interiors. These assumptions have the following implications:
   (a) In the subgrid model we require the Green's function for each element, which is easily determined for rectangular elements.
   (b) The integral operator M acting on $\bar{\phi}^h$ couples only the degrees of freedom of $\bar{\phi}^h$ within an element.

4. Numerical method

In this section we develop a numerical method based on the subgrid model developed in the previous section. We also compare the form of this approximation with other finite element methods.

Eq. (50) may be written concisely as

$$B(\bar{w}^h, \bar{\phi}^h; g^e) = L(\bar{w}^h; g^e) \tag{52}$$

where

$$B(\bar{w}^h, \bar{\phi}^h; g^e) := a(\bar{w}^h, \bar{\phi}^h) + \mathrm{i}k(\bar{w}^h, \bar{\phi}^h)_{\Gamma_h} + (\mathcal{L}\bar{w}^h, M(\mathcal{L}\bar{\phi}^h)) \tag{53}$$

$$L(\bar{w}^h; g^e) := (\bar{w}^h, f) + (\bar{w}^h, p)_{\Gamma_h} + (\mathcal{L}\bar{w}^h, M(f)) \tag{54}$$

A numerical approximation to (52) is: Find $\bar{\phi}^h \in \mathcal{S}^h$ such that

$$B(\bar{w}^h, \bar{\phi}^h; \tilde{g}^e) = L(\bar{w}^h; \tilde{g}^e) \quad \forall\, \bar{w}^h \in \bar{\mathcal{V}}^h \tag{55}$$

where $\tilde{g}^e \approx g^e$ is the approximate Green's function. We refer to the numerical method described in Eq. (55) as the *subgrid finite element method*.

The Green's function g^e for the Helmholtz operator in an interior domain with homogeneous Dirichlet boundary data is a two-point, transcendental function. In the numerical method we replace g^e by an approximate $\tilde{g}^e$ which is a two-point polynomial because this facilitates numerical integration of the matrices. The

coefficients of this polynomial are determined in terms of the moments of the Green's function. In the following subsections we derive $\tilde{g}^e$ for finite elements in one dimension and for square elements in two dimensions. We begin by transforming Eqs. (47) and (48) from global coordinates $\boldsymbol{x}$ and $\boldsymbol{x}_0$ into element coordinates $\boldsymbol{\xi}$ and $\boldsymbol{\xi}_0$, respectively.

Consider a transformation matrix $\boldsymbol{N}$ and a translation vector $\boldsymbol{t}$ defined by the relation

$$\boldsymbol{\xi} = \boldsymbol{N}\boldsymbol{x} + \boldsymbol{t} \tag{56}$$

$$\boldsymbol{\xi}_0 = \boldsymbol{N}\boldsymbol{x}_0 + \boldsymbol{t} \tag{57}$$

Then, if $\boldsymbol{N}$ has constant components, Eqs. (47) and (48) may written in element coordinates as

$$-(\nabla_{\boldsymbol{\xi}} \cdot \boldsymbol{N}\boldsymbol{N}^{\mathrm{T}}\nabla_{\boldsymbol{\xi}} + k^2) g^e(\boldsymbol{\xi}; \boldsymbol{\xi}_0) = j\delta(\boldsymbol{\xi} - \boldsymbol{\xi}_0) \quad \text{in } \Omega^e_{\mathrm{el}} \tag{58}$$

$$g^e(\boldsymbol{\xi}; \boldsymbol{\xi}_0) = 0 \quad \text{on } \Gamma^e_{\mathrm{el}} \tag{59}$$

where $j = \text{determinant}(\boldsymbol{N})$, $\nabla_{\boldsymbol{\xi}}$ is the gradient operator in $\boldsymbol{\xi}$ space, $\Omega^e_{\mathrm{el}} := \{\boldsymbol{\xi} | \boldsymbol{\xi} = \boldsymbol{N}\boldsymbol{x} + \boldsymbol{t}, \boldsymbol{x} \in \Omega_e\}$ and $\Gamma^e_{\mathrm{el}} := \{\boldsymbol{\xi} | \boldsymbol{\xi} = \boldsymbol{N}\boldsymbol{x} + \boldsymbol{t}, \boldsymbol{x} \in \Gamma_e\}$.

4.1. Approximate Green's function for a one-dimensional finite element

In one dimension $\boldsymbol{\xi} = \xi$ and $\boldsymbol{\xi}_0 = \xi_0$. We choose $\boldsymbol{N}$ and $\boldsymbol{t}$ such that $\Omega^e_{\mathrm{el}} = (-1, 1)$ for an element of length h_e. Then, Eqs. (58) and (59) specialize to

$$-\left(\frac{4}{h_e^2}\frac{\partial 2}{\partial \xi^2} + k^2\right) g^e(\xi; \xi_0) = \frac{2}{h_e}\delta(\xi - \xi_0) \quad \text{in } \Omega^e_{\mathrm{el}} \tag{60}$$

$$g^e(\xi; \xi_0) = 0 \quad \text{on } \Gamma^e_{\mathrm{el}} \tag{61}$$

Eqs. (60) and (61) may be solved (see e.g. [6]) to obtain the Green's function for the element expressed in element coordinates, viz.

$$g^e(\xi; \xi_0) = \begin{cases} \dfrac{\psi(\xi)\psi(-\xi_0)}{k\psi(1)}, & \xi < \xi_0 \\ \dfrac{\psi(-\xi)\psi(\xi_0)}{k\psi(1)}, & \xi \geq \xi_0 \end{cases} \tag{62}$$

where

$$\psi(z) = \sin(kh_e(1+z)/2) \tag{63}$$

We now approximate the function $g^e(\xi; \xi_0)$ by

$$\tilde{g}^e(\xi; \xi_0) = \sum_{i,j=0}^{1} \tau_{ij}\xi^i\xi_0^j \tag{64}$$

where

$$\tau_{ij} = \frac{\displaystyle\int_{\Omega^e_{\mathrm{el}}}\int_{\Omega^e_{\mathrm{el}}} \xi^i g^e(\xi; \xi_0)\xi_0^j \, \mathrm{d}\Omega_{\xi_0} \, \mathrm{d}\Omega_{\xi}}{\displaystyle\int_{\Omega^e_{\mathrm{el}}}\int_{\Omega^e_{\mathrm{el}}} \xi^{2i}\xi_0^{2j} \, \mathrm{d}\Omega_{\xi_0} \, \mathrm{d}\Omega_{\xi}} \tag{65}$$

Using (62) in (65) we obtain

$$\tau_{00} = \frac{1}{k}\left[\frac{2\tan(kh_e) - kh_e}{k^2h_e^2}\right] \tag{66}$$

$$\tau_{01} = \tau_{10} = 0 \tag{67}$$

$$\tau_{11} = \frac{12k}{k^3 h_e^3}\left[\frac{12 - 6kh_e\cot(kh_e) - k^2h_e^2}{k^2h_e^2}\right] \tag{68}$$

Expanding the sum in Eq. (64) we obtain the following expression for $\tilde{g}^e$

$$\tilde{g}^e(\xi;\xi_0) = \tau_{00} + \tau_{11}\xi\xi_0 \tag{69}$$

where τ_{00} and τ_{11} are defined in Eqs. (66) and (68).

4.2. Approximate Green's function for a square finite element

For a square element we let

$$\boldsymbol{\xi} = \begin{bmatrix}\xi\\ \eta\end{bmatrix} \quad \text{and} \quad \boldsymbol{\xi}_0 = \begin{bmatrix}\xi_0\\ \eta_0\end{bmatrix} \tag{70}$$

We choose N and t such that $\Omega^e_{\text{el}} = (-1,1)\times(-1,1)$ for an element with sides of length h_e. Eqs. (58) and (59) then specialize to

$$-\left(\frac{4}{h_e^2}\frac{\partial^2}{\partial\xi^2} + \frac{4}{h_e^2}\frac{\partial^2}{\partial\eta^2} + k^2\right)g^e(\xi;\xi_0) = \frac{4}{h_e^2}\delta(\xi-\xi_0)(\eta-\eta_0) \quad \text{in } \Omega^e_{\text{el}} \tag{71}$$

$$g^e(\xi;\xi_0) = 0 \quad \text{on } \Gamma^e_{\text{el}} \tag{72}$$

Eqs. (71) and (72) may be solved (see e.g. [6]) to obtain the Green's function for the element expressed in element coordinates, viz.

$$g^e(\xi,\eta;\xi_0,\eta_0) = 4\sum_{m,n=1}^{\infty}\frac{\psi_n(\xi)\psi_m(\eta)\psi_n(\xi_0)\psi_m(\eta_0)}{\pi^2(m^2+n^2) - (kh_e)^2} \tag{73}$$

where

$$\psi_p(z) = \sin\left[\frac{p\pi(1+z)}{2}\right] \tag{74}$$

We approximate the function $g^e(\xi,\eta;\xi_0,\eta_0)$ by

$$\tilde{g}^e(\xi,\eta;\xi_0,\eta_0) = \sum_{i,j,k,l=0}^{1}\tau_{ijkl}\xi^i\xi_0^j\eta^k\eta_0^l \tag{75}$$

where

$$\tau_{ijkl} = \frac{\displaystyle\int_{\Omega^e_{\text{el}}}\int_{\Omega^e_{\text{el}}}\xi^i\eta^k g(\xi,\eta;\xi_0,\eta_0)\xi_0^j\eta_0^l\,\mathrm{d}\Omega_{\xi_0}\,\mathrm{d}\Omega_\xi}{\displaystyle\int_{\Omega^e_{\text{el}}}\int_{\Omega^e_{\text{el}}}\xi^{2i}\xi_0^{2j}\eta^{2k}\eta_0^{2l}\,\mathrm{d}\Omega_{\xi_0}\,\mathrm{d}\Omega_\xi} \tag{76}$$

Using (73) in (76) we obtain the following non-zero τ_{ijkl}

$$\tau_{0000} = \frac{4^3}{\pi^4}\sum_{m,n=1}^{\infty}\frac{(2m+1)^{-2}\cdot(2n+1)^{-2}}{\pi^2[(2m+1)^2+(2n+1)^2] - (kh_e)^2} \tag{77}$$

$$\tau_{1100} = \frac{4^3 3^2}{\pi^4}\sum_{m,n=1}^{\infty}\frac{(2m)^{-2}\cdot(2n+1)^{-2}}{\pi^2[(2m)^2+(2n+1)^2] - (kh_e)^2} \tag{78}$$

$$\tau_{0011} = \tau_{1100} \tag{79}$$

$$\tau_{1111} = \frac{4^3 3^4}{\pi^4}\sum_{m,n=1}^{\infty}\frac{(2m)^{-2}\cdot(2n)^{-2}}{\pi^2[(2m)^2+(2n)^2] - (kh_e)^2} \tag{80}$$

Expanding the sum in Eq. (75) we obtain the following expression for $\tilde{g}^e$

$$\tilde{g}^e(\xi, \eta; \xi_0, \eta_0) = \tau_{0000} + \tau_{1100}(\xi\xi_0 + \eta\eta_0) + \tau_{1111}\xi\xi_0\eta\eta_0 \tag{81}$$

where τ_{0000}, τ_{1100} and τ_{1111} are defined in Eqs. (77), (78) and (80).

REMARKS

(1) The approximate Green's function $\tilde{g}^e$ for the one-dimensional element (Eq. (69)) exactly accounts for the effect of the exact Green's function on the constant and linear components of the residual in the multiscale term. Thus it is exact for an element with linear interpolations. Similarly, the approximate Green's function $\tilde{g}^e$ derived for the square element (Eq. (81)) is exact for a square element with bilinear interpolations.

(2) By substituting $\tilde{g}^e = \tau \cdot \delta(\boldsymbol{x} - \boldsymbol{x}_0)$ (where τ is an element parameter) we recover the formal Galerkin least-squares method (see [2]) from Eq. (55), viz.

$$a(\bar{w}^h, \bar{\phi}^h) + \mathrm{i}k(\bar{w}, \bar{\phi})_{\Gamma_h} + \tau(\mathscr{L}\bar{w}^h, \mathscr{L}\bar{\phi}^h) = (\bar{w}^h, f) + (\bar{w}^h, p)_{\Gamma_h} + \tau(\mathscr{L}\bar{w}^h, f) \tag{82}$$

And by substituting $\tilde{g}^e = 0$ we recover the standard Galerkin method, viz.

$$a(\bar{w}^h, \bar{\phi}^h) + \mathrm{i}k(\bar{w}, \bar{\phi})_{\Gamma_h} = (\bar{w}^h, f) + (\bar{w}^h, p)_{\Gamma_h} \tag{83}$$

5. Supercovergence of the subgrid finite element method in one dimension

In this section we prove that for certain problems in one dimension the subgrid finite element method with standard piecewise linear interpolations yields nodally exact solutions. In particular, we prove this result for Dirichlet boundary value problems involving second-order linear elliptic differential operators.

Consider the domain $\Omega = (a, b)$, a bounded, open interval on the real line. Then, $\Gamma = \{a, b\}$ is the boundary of Ω. We discretize Ω into element subdomains $\Omega^e = (x_e, x_{e+1})$ with boundaries $\Gamma^e = \{x_e, x_{e+1}\}$, $e = 1, 2, \ldots, n_{\mathrm{el}}$, where n_{el} is the number of elements. We denote by Ω' the element union of all element interiors, and by Γ' all inter-element boundaries (see Eqs. (10) and (11)).

The strong statement of the problem we wish to solve is: Find $\phi: \Omega \to \mathbb{C}$, in Ω such that

$$\mathscr{L}\phi = f \qquad \text{in } \Omega \tag{84}$$

$$\phi(a) = q_a, \qquad \phi(b) = q_b \tag{85}$$

where $\mathscr{L}$ is a second-order linear elliptic differential operator, $f: \Omega \to \mathbb{C}$, is the prescribed forcing function and q_a, $q_b \in \mathbb{C}$ are the prescribed Dirichlet boundary data. We define the operator $\mathscr{L}^*$ to be the adjoint of $\mathscr{L}$.

The equivalent weak statement of the Boundary Value Problem is: Find $\phi \in \mathscr{S}$ such that

$$a(w, \phi) = (w, f) \quad \forall\, w \in \mathscr{V} \tag{86}$$

where we define the function spaces $\mathscr{S}$ and $\mathscr{V}$ to be

$$\mathscr{S} = \{\phi \,|\, \phi \in H^1(\Omega),\ \phi(a) = q_a,\ \phi(b) = q_b\} \tag{87}$$

$$\mathscr{V} = \{w \,|\, w \in H^1(\Omega),\ w(a) = w(b) = 0\} \tag{88}$$

and $a(\cdot, \cdot)$: $\mathscr{V} \times \mathscr{S} \to \mathbb{C}$ is the sesquilinear form associated with the operator $\mathscr{L}$.

The statement of the subgrid finite element method for this problem is: Find $\bar{\phi}^h \in \bar{\mathscr{S}}^h$ such that

$$a(\bar{w}^h, \bar{\phi}^h) + (\mathscr{L}\bar{w}^h, \phi') = (\bar{w}^h, f), \quad \forall\, \bar{w}^h \in \bar{\mathscr{V}}^h \tag{89}$$

where

$$\phi'^e := \phi'(x_0)|_{\Omega^e} = -\int_{\Omega'} g^e(x; x_0)(\mathscr{L}\bar{\phi}^h - f)(x)\,\mathrm{d}x \tag{90}$$

and $g^e(x; x_0)$ is the solution to the problem:

$$\mathcal{L}^* g^e(x; x_0) = \delta(x - x_0) \quad \text{in } \Omega^e \tag{91}$$

$$g^e(x; x_0) = 0 \quad \text{on } \Gamma^e \tag{92}$$

Further by hypothesis $\phi' \in \mathcal{V}$, where

$$\mathcal{V}' = \{v \,|\, v \in H^1(\Omega); v(x) = 0, x \in \Gamma' \cup \Gamma\} \tag{93}$$

and the finite dimensional spaces $\overline{\mathcal{S}}^h$ and $\overline{\mathcal{V}}^h$ are defined as

$$\overline{\mathcal{S}}^h = \{\phi \,|\, \phi \in \mathcal{S}, \phi \in \mathcal{P}(\Omega')\} \tag{94}$$

$$\overline{\mathcal{V}}^h = \{w \,|\, w \in \mathcal{V}, w \in \mathcal{P}(\Omega')\} \tag{95}$$

where $\mathcal{P}(\Omega')$ is the space of piecewise polynomial functions of degree 1 on Ω'.

PROPOSITION 5.1. The subgrid finite element solution given by Eq. (89) is equal to the solution of the problem given by Eqs. (84) and (85) at element boundaries.

PROOF. To begin with consider the following spaces of functions.

$$\tilde{\mathcal{V}} = \{v \,|\, v = v^h + v', v^h \in \mathcal{V}^h \text{ and } v' \in \mathcal{V}'\} \tag{96}$$

$$\tilde{\mathcal{S}} = \{v \,|\, v = v^h + v', v^h \in \mathcal{S}^h \text{ and } v' \in \mathcal{V}'\} \tag{97}$$

From the definition of $\tilde{\mathcal{V}}$ we have

$$\tilde{\mathcal{V}} \subset \mathcal{V} \tag{98}$$

To prove the converse consider a function $v \in \mathcal{V}$. We construct $v^h \in \mathcal{V}$ such that $v^h|_{\Omega^e} \in \mathcal{P}(\Omega^e)$ and $v^h(x)|_{\Gamma'} = v(x)|_{\Gamma'}$. Then, by construction $v^h \in \overline{\mathcal{V}}^h$. Let $v' = v - v^h$. It is easily verified that $v' \in \mathcal{V}'$. Thus, $\forall v \in \mathcal{V}$ we have the following decomposition

$$v = v^h + v' \tag{99}$$

where $v^h \in \overline{\mathcal{V}}^h$ and $v' \in \mathcal{V}'$. Thus

$$\mathcal{V} \subset \tilde{\mathcal{V}} \tag{100}$$

From (98) and (100) we conclude

$$\tilde{\mathcal{V}} = \mathcal{V} \tag{101}$$

Also, by the definition of $\tilde{\mathcal{S}}$ we have

$$\tilde{\mathcal{S}} \subset \mathcal{S} \tag{102}$$

Now consider a function $v \in \mathcal{S}$. We construct $v^h \in \mathcal{S}$ such that $v^h|_{\Omega'} \in \mathcal{P}(\Omega')$ and $v^h(x)|_{\Gamma'} = v(x)|_{\Gamma'}$. Then, by construction $v^h \in \overline{\mathcal{S}}^h$. Let $v' = v - v^h$. It is easily verified that $v' \in \mathcal{V}'$. Thus, $\forall v \in \mathcal{S}$ we have the result

$$v = v^h + v' \tag{103}$$

where $v^h \in \overline{\mathcal{S}}^h$ and $v' \in \mathcal{S}'$. Thus

$$\mathcal{S} \subset \tilde{\mathcal{S}} \tag{104}$$

From (102) and (104) we conclude that

$$\tilde{\mathcal{S}} = \mathcal{S} \tag{105}$$

Eqs. (90), (91) and (92) imply that ϕ'^e is the solution to the problem

$$\mathcal{L}\phi'^e = -(\mathcal{L}\overline{\phi}^h - f) \quad \text{in } \Omega^e \tag{106}$$

$$\phi'^e = 0 \quad \text{on } \Gamma^e \tag{107}$$

Summing the Euler–Lagrange equations associated with (106) and (107) for all the elements $e = 1, \ldots, n_{el}$, we obtain:

$$(w', \mathcal{L}\phi' + \mathcal{L}\bar{\phi}^h - f)_{\Omega'} = 0 \quad \forall\, w' \in \mathcal{V}' \tag{108}$$

Integrating by parts in Eqs. (89) and (108) we arrive at an alternative statement for the subgrid finite element method, viz. Find $\bar{\phi}^h \in \bar{\mathcal{S}}^h$ such that

$$a(\bar{w}^h, \bar{\phi}^h) + a(\bar{w}^h, \phi') = (\bar{w}^h, f), \quad \forall\, \bar{w}^h \in \bar{\mathcal{V}}^h \tag{109}$$

where $\phi' \in \mathcal{V}'$ satisfies

$$a(w', \bar{\phi}^h) + a(w', \phi') = (w', f), \quad \forall\, w' \in \mathcal{V}' \tag{110}$$

Eqs. (109) and (110) may be written concisely as: Find $\tilde{\phi} \in \tilde{\mathcal{S}}$ such that

$$a(\tilde{w}, \tilde{\phi}) = (\tilde{w}, f), \quad \forall\, \tilde{w} \in \tilde{\mathcal{V}} \tag{111}$$

where $\tilde{\phi} = \bar{\phi}^h + \phi'$ and $\tilde{w} = \bar{w}^h + w'$.

Using results (101) and (105) in Eq. (111) we recover the weak form of the BVP. Thus, $\tilde{\phi}$ satisfies the weak form of the problem. From the equivalence of the weak and the strong form of the problem we conclude that $\tilde{\phi}$ is the solution to Eqs. (84) and (85), therefore

$$\tilde{\phi} = \phi \tag{112}$$

Now, since $\tilde{\phi} = \bar{\phi}^h + \phi'$ and $\phi' = 0$ on $\Gamma' \cup \Gamma$ by hypothesis, we have

$$\bar{\phi}^h = \phi \quad \text{on } \Gamma' \cup \Gamma \tag{113}$$

That is, the subgrid finite element solution is equal to the exact solution of the given problem at element boundaries. □

REMARKS

(1) As a consequence of Proposition 5.1, we observe that for linear elements in one dimension the subgrid finite element solution will be nodally exact.

(2) Proposition 5.1 is valid only for problems in one dimension. For multi-dimensional problems the spaces corresponding to $\bar{\mathcal{V}}$ and $\bar{\mathcal{S}}$ are not equal to $\mathcal{V}$ and $\mathcal{S}$, respectively, and hence the proof described above is no longer valid.

6. Numerical examples

In this section we evaluate the performance of the subgrid finite element method (SFEM) given by Eq. (55). The approximate Green's function $\tilde{g}^e$ employed in Eq. (55) is given by Eq. (69) in one dimension and by (81) in two dimensions. We compare the performance of this method with

(1) The standard Galerkin method (Eq. (83)).

(2) The Galerkin least squares method (Eq. (82)). For problems in one dimension, the value of the mesh parameter τ used is taken from [2]. For problems in two dimensions we have used the $\tau_{22.5}$ defined in [7] as the optimal mesh parameter τ in our GLS solution.

The strong form of the model problems is given by Eqs. (1) through (3). For evaluating finite element solutions for all the problems, we employ standard piecewise linear (bilinear in two dimensions) approximations.

6.1. One-dimensional problem on a non-uniform mesh

Here, the domain $\Omega = (0, 1)$ and the boundary $\Gamma = \{0, 1\}$. We prescribe only Dirichlet boundary conditions for this problem, therefore $\Gamma_q = \Gamma$ and $\Gamma_h = \emptyset$. The forcing function $f = 0$ and the prescribed Dirichlet boundary data is $\phi(0) = 0$, $\phi(1) = 1$. We employ a non-uniform finite element mesh, and solve the problem for $kh_{\max} = 1.6$ and 2.4, where k is the wavenumber for the problem and $h_{\max}$ is the length of the largest element. We observe:

(1) For $kh_{\max} = 1.6$ (see Fig. 2) the standard Galerkin method is inaccurate. The GLS solution is much more accurate but it displays some error in amplitude. The SFEM solution is pointwise exact. This verifies the observation made in Section 5.

(2) For $kh_{\max} = 2.4$ (see Fig. 3), which corresponds to a very coarse resolution, we compare only the GLS and SFEM solutions. The GLS solution is highly inaccurate while the SFEM solution continues to be pointwise exact.

6.2. One-dimensional problem with a non-zero source term

Here, the domain $\Omega = (0, 1)$, the boundary $\Gamma = \{0, 1\}$. Again, since we prescribe only Dirichlet boundary conditions and therefore $\Gamma_q = \Gamma$ and $\Gamma_h = \emptyset$. The prescribed Dirichlet boundary data is $\phi(0) = 0$, $\phi(1) = 0$ and the forcing function f is defined by

$$f(x) = \begin{cases} 1, & x < 0.5 \\ 1 - (x - 0.5)/0.1, & 0.5 \leq x \leq 0.6 \\ 0, & x > 0.6 \end{cases} \tag{114}$$

For this problem we discretize the domain into 10 elements of equal length h, and evaluate the numerical solutions for $kh = 1.6$ and 2.4. The results are shown in Figs. 4 and 5. As in the previous problem, nodal exactness is obtained with the SFEM method.

6.3. Green's function problem in two dimensions

For this problem the domain $\Omega = (0, L) \times (0, L)$ is a square with sides of length $L = 1$. The boundary Γ is given by $\Gamma = \Gamma^1 \cup \Gamma^2 \cup \Gamma^3 \cup \Gamma^4$ where,

$$\Gamma^1 = [x, 0], \quad x \in [0, 1] \tag{115}$$

$$\Gamma^2 = [1, y], \quad y \in [0, 1] \tag{116}$$

$$\Gamma^3 = [x, 1], \quad x \in [0, 1] \tag{117}$$

$$\Gamma^4 = [0, y], \quad y \in [0,1] \tag{118}$$

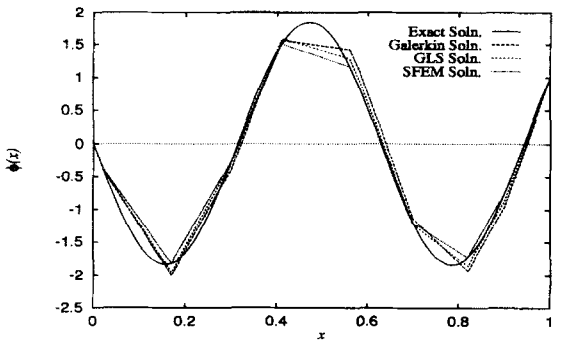

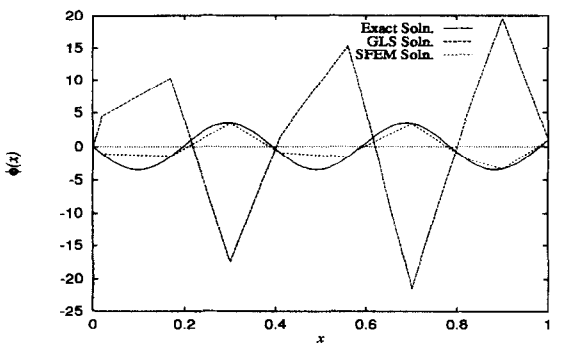

Fig. 2. Non-uniform mesh, $kh_{\max} = 1.6$.

Fig. 3. Non-uniform mesh, $kh_{\max} = 2.4$.

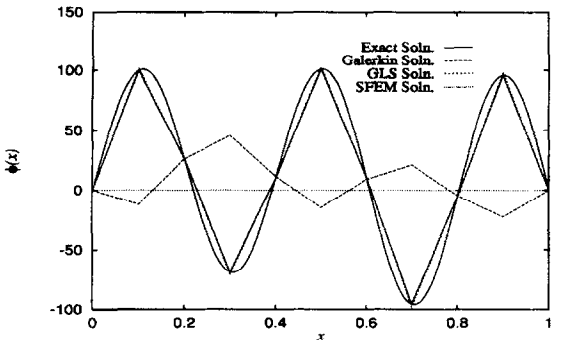

Fig. 4. Non-zero forcing function, $kh = 1.6$.

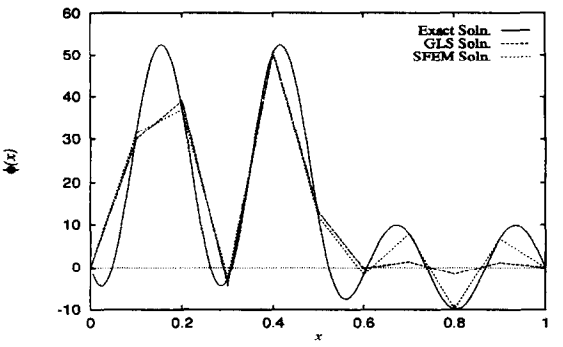

Fig. 5. Non-zero forcing function, $kh = 2.4$.

The forcing function $f = \delta(x - x_0)(y - y_0)$ is a Dirac delta function located at $(x_0, y_0) = (0.1875, 0.1875)$. Since we prescribe Dirichlet boundary conditions all along the boundary, we have $\Gamma_q = \Gamma$ and $\Gamma_h = \emptyset$. The prescribed Dirichlet boundary data is $\phi(x, y) = 0$ on Γ. The non-dimensional wavenumber associated with the problem is $kL = 8$.

The analytical solution to the problem is given by

$$\phi(x, y; x_0, y_0) = 4 \sum_{m,n=1}^{\infty} \frac{\psi_n(x)\psi_m(y)\psi_n(x_0)\psi_m(y_0)}{\pi^2(m^2 + n^2) - k^2} \quad x, y \in \Omega \tag{119}$$

where

$$\psi_p(z) = \sin(p\pi z) \tag{120}$$

As shown in Fig. 6, this solution represents a complex pattern of standing waves with a singularity at (x_0, y_0).

We discretize the domain uniformly into 64 square elements and compare the performance of Galerkin and subgrid finite element methods. For the SFEM solution we use the coarse scale solution (i.e. $\bar{\phi}^h$) to obtain the fine scale solution using Eq. (49) and treat their sum as the complete SFEM solution. Fig. 7 is a plot of the exact and the numerical solutions along the x axis at a constant value of $y = y_p = 0.190625$. We observe that the exact solution displays a spike close to the point source. Away from this region both numerical methods are fairly accurate. But around this region the Galerkin method appears to be in need of significant mesh refinement to capture the behavior of the exact solution. The SFEM solution, however, captures the spike accurately. Fig. 8 illustrates how the multiscale construct works for this example. In this figure we have plotted the coarse scale and the total SFEM solution and compared them with the exact solution. It can be seen that the fine scale contribution adds to the coarse scale solution within each element to make it more accurate.

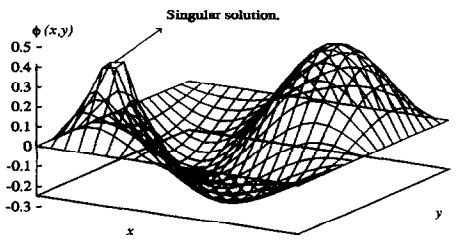

Fig. 6. Green's function problem. Exact solution.

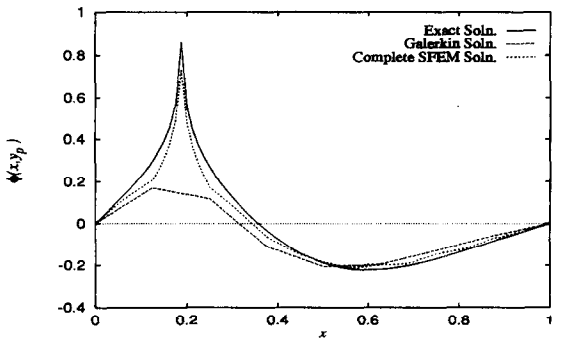

Fig. 7. Green's function problem. Solution at $y = y_p$.

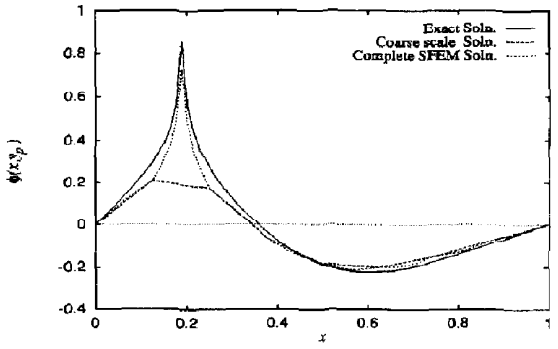

Fig. 8. Green's function problem. Solution at $y = y_p$.

6.4. Wave propagation in two dimensions

The problem of wave propagation is inherently different from the three numerical problems we have studied so far. This problem involves a mixed boundary condition which allows transmission of certain waves across the boundary. The domain of our problem is $\Omega = (0, L) \times (0, L)$ with $L = 1$ and the boundary is given by $\Gamma = \Gamma^1 \cup \Gamma^2 \cup \Gamma^3 \cup \Gamma^4$. The segments Γ^1, Γ^2, Γ^3 and Γ^4 are defined in Eqs. (115) through (118). Since the boundary condition is of a mixed type $\Gamma_q = \emptyset$ and $\Gamma_h = \Gamma$. The mixed boundary condition is given by Eq. (3), wherein the function p is given by

$$p(x, y) = \begin{cases} \mathrm{i}(k - k_y)\exp(\mathrm{i}k_x x) & (x, y) \in \Gamma^1 \\ \mathrm{i}(k + k_x)\exp(\mathrm{i}k_x + \mathrm{i}k_y y) & (x, y) \in \Gamma^2 \\ \mathrm{i}(k + k_y)\exp(\mathrm{i}k_x x + \mathrm{i}k_y) & (x, y) \in \Gamma^3 \\ \mathrm{i}(k - k_x)\exp(\mathrm{i}k_y y) & (x, y) \in \Gamma^4 \end{cases} \tag{121}$$

where

$$(k_x, k_y) = k(\cos\theta, \sin\theta) \tag{122}$$

The exact solution to the problem is a plane wave of the form

$$\phi(x, y) = \exp(\mathrm{i}kx\cos\theta + \mathrm{i}ky\sin\theta) \quad x, y \in \Omega \tag{123}$$

where θ is the angle of propagation of the wave. For our model problem we first choose $\theta = \pi/4$ and then $\theta = 0$ radians.

We discretize the domain uniformly with square elements and solve the problem at four different values of kL ($L = 1$ in each case) keeping kh fixed at 1.0 (h is the length of the side of each square element).

We use the results of this problem to quantify error due to pollution in each of the numerical methods. The pollution effect is defined in [1] as follows. Let

$$e = \frac{\|\phi - \bar{\phi}^h\|}{\|\phi\|} \tag{124}$$

where $\|\cdot\|: H^1(\Omega) \to \mathbb{R}$, is the L^2 norm defined as

$$\|\phi\| := (\phi, \phi)^{1/2} \tag{125}$$

If, for a numerical method

$$e \geqslant (kL)^{\alpha}(kh)^{s} \quad \text{where } \alpha > 0 \tag{126}$$

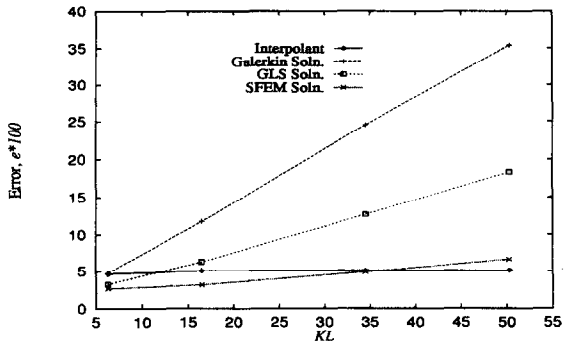

Fig. 9. Pollution error for the plane wave problem. $\theta = \pi/4$.

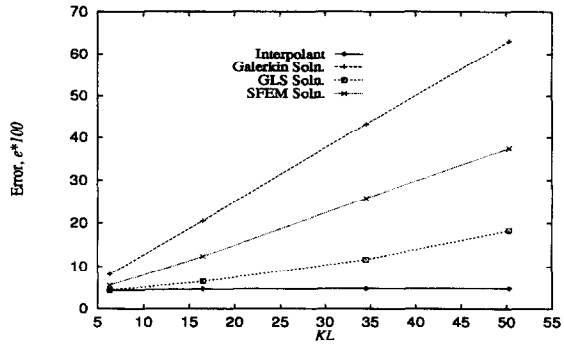

Fig. 10. Pollution error for the plane wave problem. $\theta = 0$.

then the method is said to display a pollution effect. Eq. (126) implies that for identical discretizations (kh = constant) the error in the solution increases as the wavenumber increases.

Fig. 9 shows the error of Galerkin, GLS and the subgrid finite element solutions as a function of the non-dimensional wavenumber (kL) for $\theta = \pi/4$. We observe that the SFEM solution displays significantly less pollution than the Galerkin and the GLS methods.

Fig. 10 is the same plot but with $\theta = 0$. In this plot we observe that the SFEM solution shows less pollution than the Galerkin solution but is worse than the GLS solution. Thus, for pollution error the SFEM solution displays a drawback in that the accuracy of the method is dependent on the direction of propagation of the wave.

7. Conclusions

For the Helmholtz equation we have successfully developed and implemented a subgrid finite element method based on a general multiscale variational equation. In one dimension we have proved and then verified that this method is superconvergent. In two dimensions we have shown how this method may be utilized to resolve subgrid phenomena.

In order to effectively address error due to the pollution effect in multi-dimensions, it is necessary to remove the restriction that the fine scales vanish on element boundaries, viz. Eq. (37). The authors are currently exploring the possibility of developing and implementing a numerical method derived from the multiscale variational formulation, i.e. Eq. (32) which does not impose this constraint on the fine scales [5].

Acknowledgements

The authors would like to thank Professor T.J.R. Hughes for his valuable assistance in this work and also the U.S. Office of Naval Research (ONR) for their support through grant N00014-96-10109.

References

[1] I. Babuška, F. Ihlenburg, E.T. Paik and S.A. Sauter, A generalized finite element method for solving the Helmholtz equation in two dimensions with minimal pollution, Comput. Methods Appl. Mech. Engrg. 128 (1995) 325–359.

[2] I. Harari and T.J.R. Hughes, Galerkin/least-squares finite element methods for the reduced wave equation with non-reflecting boundary conditions in unbounded domains, Comput. Methods Appl. Mech. Engrg. 98 (1992) 411–454.

[3] T.J.R. Hughes, Multiscale phenomena: Green's functions, the Dirichlet-to-Neumann formulation, subgrid scale models, bubbles, and the origins of stabilized methods, Comput. Methods Appl. Mech. Engrg. 129 (1995) 387–401.

[4] T.J.R. Hughes, G.R. Feijóo, L. Mazzei and J.-B. Quincy, The variational multiscale method—a paradigm for computational mechanics, in preparation.

[5] A.A. Oberai and P.M. Pinsky, Finite element methods for the Helmholtz equation based on global multiscale variational forms, in preparation.
[6] G.F. Roach, Green's Functions, 2nd edition (Cambridge University Press, New York, 1982).
[7] L.L. Thompson and P.M. Pinsky, A Galerkin least-squares finite element method for the two-dimensional Helmholtz equation, Int. J. Numer. Methods Engrg. 38 (1995) 371–397.